Multicomponent inclusions in Nacken synthetic emeralds

Dr Karl Schmetzer[1], Dr Lore Kiefert[2] and Dr Heinz-Jürgen Bernhardt[3]

1. Marbacher Strasse 22b, D-85238 Petershausen, Germany
2. SSEF Swiss Gemmological Institute, Falknerstr. 9, CH-4001 Basel, Switzerland
3. Institut für Mineralogie, Ruhr-Universität, D-44780 Bochum, Germany

ABSTRACT: Multicomponent inclusions in Nacken synthetic emeralds were examined by a combination of microscopy, electron microprobe analysis and micro-Raman spectroscopy. The tiny crystals at the widest ends of nailhead spicules are most probably beryl. Various forms of cavities contain single component and multicomponent fillings, which were determined as a solidified melt consisting of the ingredients of beryl and residues of a molybdenum- and vanadium-bearing flux. The residual slightly inhomogeneous melt trapped in elongated cavities is partly unmixed and contains polymerized and non-polymerized molybdates as well as Si–O–Si networks and isolated SiO_4 tetrahedra. Similar inclusions in Chatham synthetic emeralds are also characterized.

Keywords: Chatham, crystal growth, electron microprobe analyses, multi-component inclusions, Nacken, nailhead spicules, Raman spectra, synthetic emerald

Introduction

Nacken synthetic emeralds were grown in the 1920s by Professor R. Nacken of Frankfurt, Germany, and were regarded as hydrothermally grown synthetic emeralds for almost half a century (Van Praagh, 1946, 1947; Webster, 1955, 1958; Eppler, 1958; Espig, 1962; Landais, 1971; see also Schmetzer and Kiefert, 1998). This view was also confirmed by the examination with modern analytical techniques such as infrared spectroscopy which revealed the presence of characteristic water absorption bands of hydrothermally-grown synthetic emeralds (Landais, 1971). A detailed study by Nassau (1976, 1978, 1980), however, showed that two different types of Nacken synthetic emeralds were grown, both by the flux method. The first type of crystal contained irregularly shaped seeds of natural, colourless beryl, and the second type was grown without natural seeds.

The examination of both types of Nacken synthetic emerald by Nassau (1976, 1978, 1980) revealed the presence of water absorption bands in the spectra of the first type samples, which are caused by the water content of the natural beryl seed. In contrast, infrared spectra of samples of the second type of Nacken synthetic emeralds showed an absorption spectrum without any water related absorption bands, which is typical for flux-grown synthetic emeralds. These results are also useful to understand the earlier examinations by Landais (1971) using infrared spectroscopy, who, most probably, investigated samples of the first type with a natural beryl seed (Landais, 1998).

 ISSN: 1355–4565

Chemical investigations by Nassau (1978, 1980) proved that the flux used by Nacken was a molybdenum- and vanadium-bearing compound, most probably a lithium-containing oxide of a general formula MoO_3–V_2O_5–Li_2O, whose exact composition is still unknown. The X-ray fluorescence spectrum of characteristic inclusions was examined in the scanning electron microscope (SEM-EDXRF). With this technique, however, the presence of light elements such as lithium and beryllium cannot be determined. The experimental conditions applied by Nassau (1978, 1980) allowed the examination of the material trapped within various cavities alone, i.e. the X-ray fluorescence spectra represented only substances trapped in cavities without any contributions of the synthetic emerald host to the X-ray fluorescence patterns obtained (Nassau, 1998).

Two types of patterns were described consisting of the characteristic X-ray lines of (a) an Al–Si–V–Mo-bearing compound and (b) an Al–Si–V–Cr–Mo-bearing compound.

These results indicate that the material trapped within the cavities consists of a mixture of the components of beryl (BeO, Al_2O_3, SiO_2) with different percentages of chromium and of components of the flux (most probably MoO_3, V_2O_5, Li_2O). The material in the cavities was assumed to be in the vitreous state (Nassau, 1978, 1980, 1998).

Occasionally, inclusions that form elongated spicules with a tiny crystal at their widest ends are present in Nacken synthetic emeralds. These tiny crystals were described as phenakite by Nassau (1978), which is not consistent with the description of Eppler (1958), who assumed tiny beryl crystals being present as nailheads in Nacken synthetic emeralds. Both determinations, however, were based on visual appearance only and not on direct analytical measurements.

Tiny crystals at the base of nailhead spicules are common in hydrothermal synthetic emeralds, but may also form in flux-grown synthetic emerald when growth is started on a seed plate inclined at an angle to the *c*-axis (Flanigen *et al.*, 1967). In hydrothermal synthetic emeralds, these tiny crystals at the widest ends of elongated spicules were regarded exclusively as phenakite crystals for a long time. It was proven by micro-Raman spectroscopy, however, that not only phenakite but beryl and chrysoberyl crystals could also be present at the ends of elongated spicules in hydrothermal synthetic emerald from different producers (Schmetzer *et al.*, 1997). Continuing the study of nailhead spicules in synthetic emeralds, the authors have tried to determine experimentally the identity of the nailhead crystals present in these typical inclusions of Nacken synthetic emeralds and

Figure 1a,b: *Nacken synthetic emerald crystals with natural seeds (a) and without natural seeds (b). The largest crystals of both types measure about 5.5 x 4 mm (photos: M. Glas).*

a

b

to evaluate the discrepancy between the papers of Eppler (1958) and Nassau (1978). In addition, the identification of various substances present in the cavities of Nacken synthetic emeralds has been attempted.

Materials and methods

The present study is based on the examination of 14 individual samples (*Figures 1a, b*) ranging from 5.5 to 2 mm in size. The synthetic emeralds originated from the following collections: E. Gübelin, Lucerne, Switzerland (5); F.H. Pough, Reno, Nevada, USA (8); M. Schaeffer, Detmold, Germany (1).

For assessing the study of Eppler (1958), Nacken synthetic emeralds of the Gübelin collection have been available. The papers of Nassau (1976, 1978, 1980) were based on samples of the Pough collection and on synthetic emeralds from the British Museum (Natural History), London. The present authors tried to obtain the Nacken synthetic emeralds kept in the British Museum for comparison, but these samples were not made available.

For the examination of chemical properties of the substances trapped in elongated spicules and/or channels parallel to the *c*-axis, one sample without a microscopically visible colourless seed was sawn into two parts along the *c*-axis and subsequently polished down step by step. In some of these steps several elongated cavities were carefully opened and the inclusions exposed to the surface were examined by electron microprobe.

To determine the compositions of nailhead crystals at the widest ends of elongated spicules as well as individual components or phases trapped in different cavities of Nacken synthetic emeralds, numerous inclusions in both types of samples (with and without colourless seeds) were examained by micro-Raman spectroscopy. This technique, which is useful for the determination of inclusions in natural and synthetic emeralds (Schmetzer *et al.*, 1997; Schmetzer and Kiefert, 1998; Zwaan and Burke, 1998), is also a very sensitive tool for determining the substances present in

Figure 2: *Prismatic crystal of Nacken synthetic emerald which contains a colourless, natural irregularly-shaped seed; the c-axis runs vertically, melt filled channels and spicules are oriented parallel to c. Immersion, length of crystal 2 mm.*

artificially filled fissures of natural emeralds (Hänni *et al.*, 1997). Micro-Raman spectroscopy has been used by Delé-Dubois *et al.* (1986) as well as Delé-Dubois and Poirot (1989) for the determination of residual substances in synthetic emeralds. In these papers, the materials trapped in various cavities of flux-grown synthetic emeralds were determined as polymolybdates and molybdenum oxides.

Microscopic properties

The microscopic examination confirmed the results of Nassau (1976, 1978, 1980), who classified the 19 synthetic emeralds available for his study into two groups with and without natural seeds.

In our 14 samples, colourless, natural irregularly shaped seeds were observed in eight synthetic emeralds (*Figures 2 and 3*). In two of these crystals, thin, flat cavities oriented on planes parallel to the basal pinacoid were observed (*Figure 3*). These

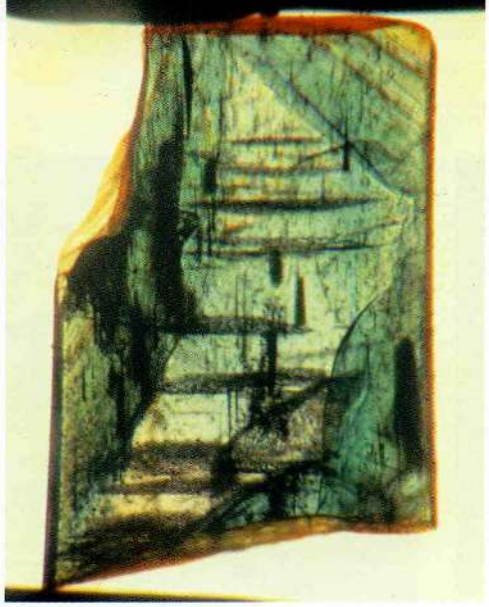

Figure 3: *Prismatic crystal of Nacken synthetic emerald which contains a colourless, natural irregularly shaped seed; the c-axis runs vertically, melt filled channels and spicules are oriented parallel to c, flat cavities with primary liquid and two-phase inclusions are oriented perpendicular to c. Immersion, length of crystal. 3.4 mm.*

cavities contain primary liquid and/or two-phase inclusions, which is a typical microscopic feature for natural beryl or natural emerald from certain localities, e.g. Russian Uralian emeralds (see Schmetzer *et al.*, 1991).

In the remaining six of our Nacken samples, no colourless irregularly shaped seeds were observable by microscopic examination. One larger synthetic emerald crystal of this group was examined by infrared spectroscopy, which showed the absence of water-related absorption bands. Again, these results are consistent with the findings described by Nassau (1978, 1980).

All Nacken synthetic emeralds revealed numerous channels or spicules oriented parallel to the *c*-axis (*Figures 2 and 3*), which are more or less opaque in transmitted light (*Figure 4a*). Nailhead spicules, i.e. elongated spicules with tiny crystals at their widest ends, are common in samples with colourless seeds, but rare in the second group of synthetic emeralds without colourless natural seeds. The tiny birefringent crystals have a refractive index close to that of the host synthetic emerald, so they can be difficult to observe without crossed polarizers (*Figure 4a, b*). In samples with colourless seeds, most of these tiny birefringent crystals were in direct contact with the irregularly shaped surface of the seed. The narrower ends of the spicules always pointed in the direction of growth parallel to the *c*-axis of the synthetic emerald crystals. Occasionally, nailhead spicules were seen on two opposite surfaces of the seed with their tips pointing in opposite directions up and down along the *c*-axis (*Figure 5*).

The material trapped in the channels and spicules appeared inhomogeneous under the microscope. In addition to a shrinking bubble, which was frequently oberved, several yellow, yellowish or whitish, transparent or translucent substances were

Figure 4a, b: *Nailhead spicules in Nacken synthetic emerald: the tiny beryl crystals at the wider ends of the spicules display a low relief in plane polarized light (a), the birefringent crystals are clearly visible with crossed polarizers (b; right), Immersion 100x.*

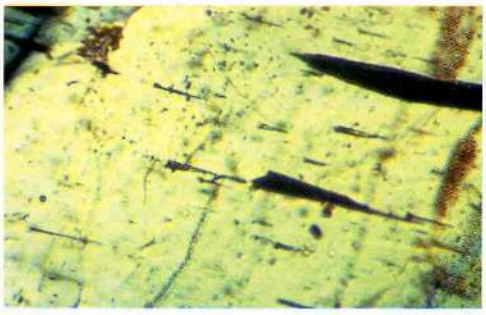

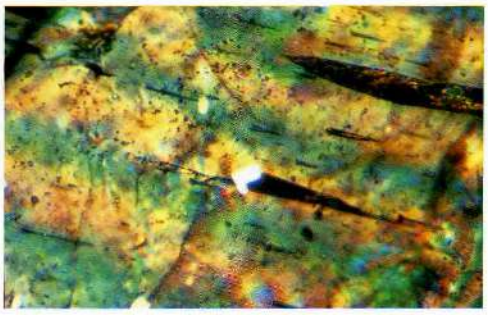

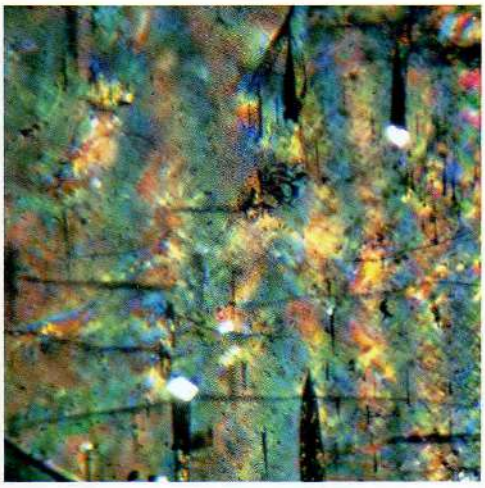

Figure 5: *Nailhead spicules in Nacken synthetic emerald: the c-axis runs vertically, the narrower ends of the spicules point towards the directions of growth up and down along the c-axis, the tiny beryl crystals at the wider ends of the spicules are in direct contact with two irregularly-shaped surfaces of a colourless beryl seed in the centre of the crystal. Immersion, crossed polarizers. 60x.*

often present (*Figures 6, 7 and 8*). Only in a few cases did a single cavity appear to be homogeneously filled with one single phase or component.

Determination of birefringent crystals at the widest ends of cone-shaped spicules

Numerous nailheads at the widest ends of elongated spicules (*Figures 4, 5 and 6*) in different samples were examined by micro-Raman spectroscopy. In all cases, we obtained Raman spectra of beryl only; no spectra indicating phenakite were recorded. The authors have identified nailhead spicules in hydrothermal synthetic emeralds from various producers (Schmetzer *et al.*, 1997) and have used the same experimental conditions in the present investigation; they are confident that if the spicules had been anything other than beryl they would have been detected by the Raman microprobe. Consequently, the birefringent crystals at the ends of cone-shaped spicules are most

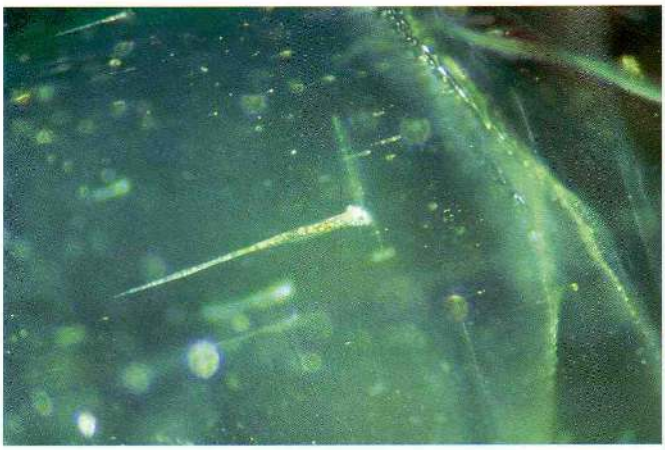

Figure 6: *Nailhead spicule with multicomponent filling in Nacken synthetic emerald. 100x.*

Figure 7: *Elongated spicule with multicomponent filling in Nacken synthetic emerald. 100x.*

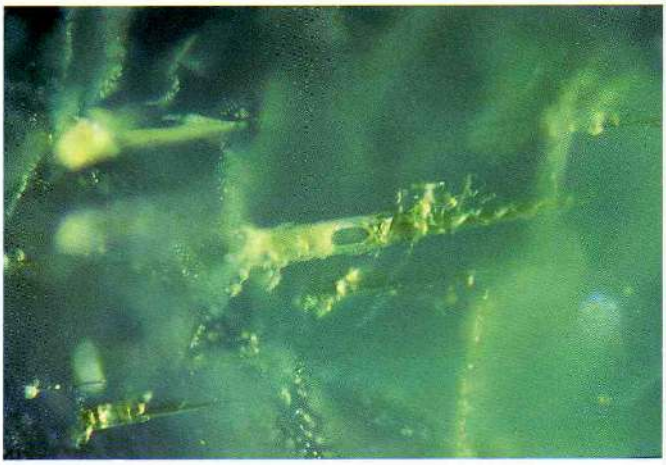

Figure 8: *Elongated channel parallel to the c-axis with multicomponent filling and shrinking bubble. Renishaw Raman microscope. 200x.*

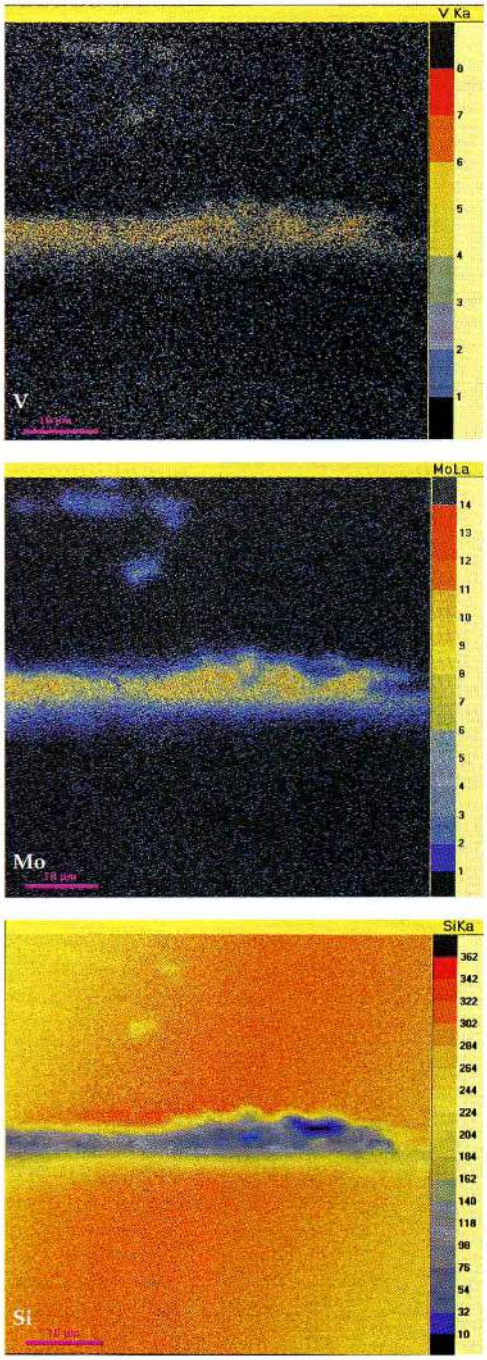

Figure 9a, b, c: *Element distribution maps obtained by electron microprobe analysis showing a slightly inhomogeneous distribution of Si, Mo and V as components of residual melt trapped in a channel parallel to the c-axis.*

probably tiny beryl crystals whose orientation is different from that of the host synthetic emerald.

Examination of multicomponent inclusions in elongated cavities

Microprobe analyses showed that the substances trapped in various cavities (*Figures 6, 7 and 8*) revealed the characteristic X-ray lines of Al, Si, V, Cr and Mo. Consequently, these cavities contain the ingredients of emerald (Al, Si, Cr) and residual quantities of the flux (Mo, V). Furthermore, neither sodium nor potassium was found in the cavities. These chemical data are consistent with the analytical results of Nassau (1978, 1980).

Although element distribution maps for some cavities (*Figure 9a, b and c*) revealed various inhomogeneities, no different phases or distinct phase boundaries between different chemical compounds were seen. No individual areas which consisted only of clearly resolved silicates without components of the flux (molybdenum and vanadium) or which consisted of only molybdenum and/or vanadium without any silicon were observed.

In Nacken synthetic emeralds, several basic types of Raman spectra were obtained from the material trapped in various cavities. No differences were observed relating specifically to sample type. For individual areas of different cavities, similar spectra were observed in some cases, but varying types of spectra were commonly obtained from different areas within one single cavity.

The most simple and frequently measured spectrum consisted of a single Raman line at about 956 cm^{-1} with a shoulder at about 871 cm^{-1} (*Figure 10a*). Other parts of the inclusions gave more complex spectra containing two additional lines at 830 cm^{-1} and in the 425 to 435 cm^{-1} range (*Figure 10b*) and in most cases, a line at about 714 cm^{-1} was also present (*Figure 10c, d and e*). Less commonly, two lines at 894 cm^{-1} and in the 313 to 320 cm^{-1} range were observed.

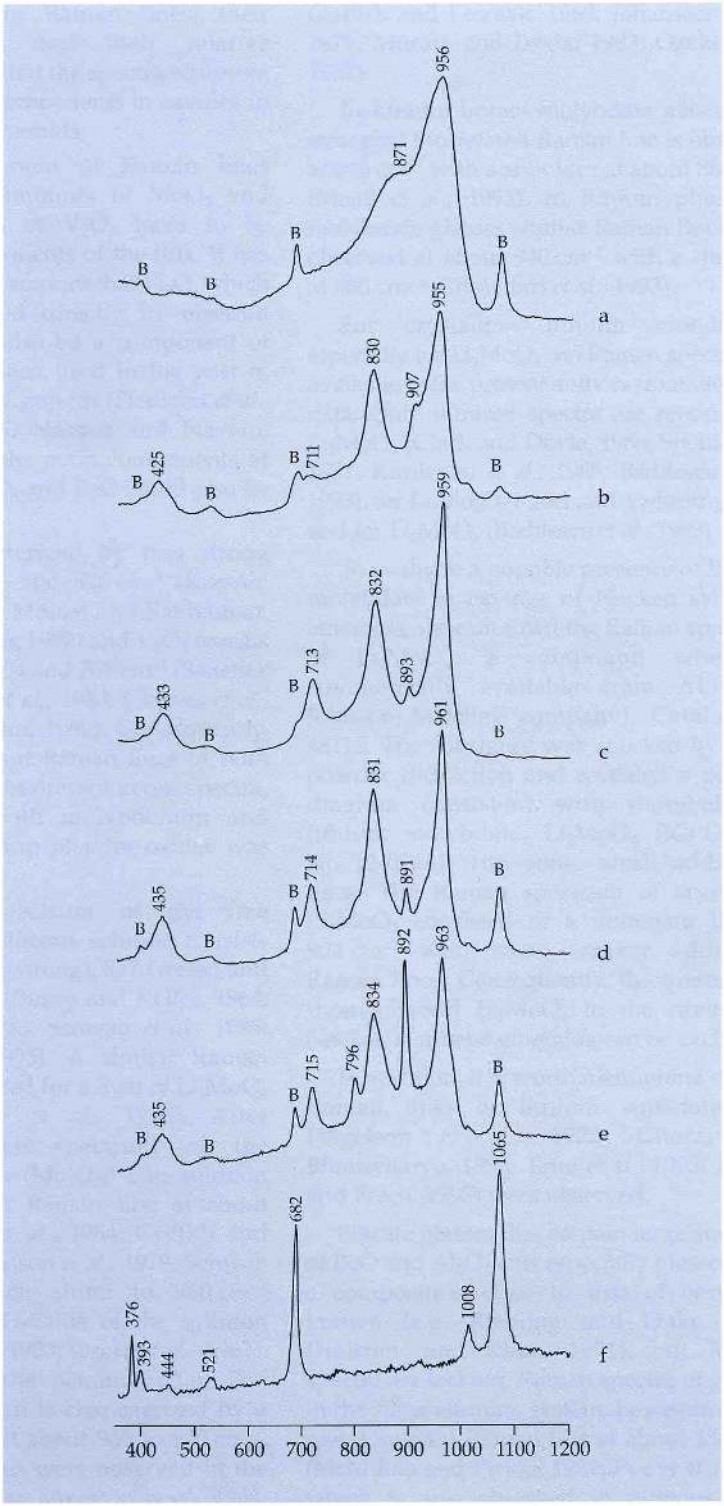

Figure 10: *Typical Raman spectra obtained from multicomponent inclusions in spicules or channels parallel to the c-axis of Nacken synthetic emerald crystals; the inclusions consist of residues of a molybdenum- and vanadium-bearing flux and the ingredients of beryl; in spectra 10a to 10e the positions of Raman lines of the host beryl are indicated by B: 10f is a Raman spectrum of the beryl host alone.*

The variation in Raman lines, their possible overlaps and their relative intensities, indicate that the spectra represent several individual components in cavities in Nacken synthetic emeralds.

For the assignment of Raman lines measured, major amounts of MoO_3 and minor percentages of V_2O_5 have to be considered as components of the flux. It has also to be taken into account that Li_2O, which cannot be measured directly by electron microprobe, could also be a component of the flux as it has been used in the past in solvents for emerald growth (Flanigen *et al.*, 1967; Nassau, 1976; Nassau and Nassau, 1980). In addition, the main components of beryl, i.e. SiO_2, Al_2O_3 and BeO could also be present in the melt.

MoO_3 is characterized by two strong Raman lines at 996 and 826 cm^{-1} (Krasser, 1969; Py *et al.*, 1977; Mohan and Ravikumar, 1984; Hirata and Zhu, 1992) and V_2O_5 reveals two strong lines at 994 and 701 cm^{-1} (Sanchez *et al.*, 1982; Abello *et al.*, 1983; Clauws *et al.*, 1985; Hirata and Zhu, 1992). Consequently, because the dominant Raman lines of both oxide phases were not present in our spectra, the presence of both molybdenum and vanadium in the form of pure oxides was excluded.

The Raman spectrum of the free molybdate ion in aqueous solution consists of three lines at 897 (strong), 837 (weak) and 317 cm^{-1} (medium) (Busey and Keller, 1964; Weinstock *et al.*, 1973; Schwab *et al.*, 1985; Pope and West, 1995). A similar Raman spectrum was reported for a melt of Li_2MoO_4 in K_2MoO_4 (Cape *et al.*, 1976). After polymerization, the spectrum of the heptamolybdate ion ($Mo_7O_{24}^{6-}$) in solution reveals a dominant Raman line at about 940 cm^{-1} (Aveston *et al.*, 1964; Griffith and Lesniak, 1969; Johansson *et al.*, 1979; Schwab *et al.*, 1985), which shifts to 960 cm^{-1} according to the pH-value of the solution (Murtaa and Ikeda, 1983; Ozeki *et al.*, 1987). The spectrum of the octomolybdate ion ($Mo_8O_{26}^{4-}$) in solution is characterized by a strong Raman line at about 960 to 970 cm^{-1}, in solids several lines were observed in the 920 to 970 cm^{-1} range (Aveston *et al.*, 1964; Griffith and Lesniak, 1969; Johansson *et al.*, 1979; Murata and Ikeda, 1983; Ozeki *et al.*, 1987).

In lithium borate molybdate glasses, the strongest Mo-related Raman line is observed at 940 cm^{-1} with a shoulder at about 880 cm^{-1} (Maaß *et al.*, 1993). In lithium phosphate molybdate glasses similar Raman lines were observed at about 940 cm^{-1} with a shoulder at 880 cm^{-1} (Chowdari *et al.*, 1993).

For crystalline lithium molybdates, especially for Li_2MoO_4, no Raman spectrum is available to the present authors from literature data. Only infrared spectra are reported for Li_2MoO_4 (Clark and Doyle, 1966; Spoliti *et al.*, 1981; Kurilenko *et al.*, 1988; Badilescu *et al.*, 1993), for $Li_2Mo_2O_7$ (Goel and Mehrotra, 1985) and for Li_2MoO_3 (Badilescu *et al.*, 1993).

To evaluate a possible presence of lithium molybdate in cavities of Nacken synthetic emeralds, we examined the Raman spectrum of Li_2MoO_4, a compound which is commercially available from ALFA (a Johnson Matthey company), Catalog-No. 48115. The substance was checked by X-ray powder diffraction and revealed a powder diagram consistent with rhombohedral lithium molybdate, Li_2MoO_4 (JCPDS file No. 12-0763) with some weak additional lines. The Raman spectrum of crystalline Li_2MoO_4 consisted of a dominant line at 904 cm^{-1} with some weaker additional Raman lines. Consequently, the presence of rhombohedral Li_2MoO_4 in the cavities of Nacken synthetic emeralds can be excluded.

In addition, it is worth mentioning that no Raman lines of lithium vanadate (see Feigelson *et al.*, 1972; Ghorai and Bhattacharya, 1995; Tang *et al.*, 1995; Zhang and Frech, 1997) were observed.

Silicate glasses that contain large amounts of BeO and Al_2O_3 and especially glasses with a composition close to that of beryl are known (e.g. Riebling and Duke, 1967; Dmitriev and Khan, 1971), but Raman spectra are lacking. Raman spectra of glasses in the silica-alumina system, however, reveal one dominant Raman line at about 430 cm^{-1} (McMillan and Piriou, 1982; Poe *et al.*, 1992), which is also observed in vitreous silica

Chatham flux grown synthetic emeralds

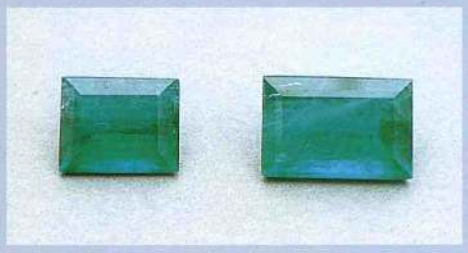

Figure 11: *Two faceted Chatham synthetic emeralds; sizes of the samples 9.1 x 7.3 mm and 11.4 x 7.7 mm (photo: H.A. Hänni).*

During the examination of nailhead spicules in hydrothermal synthetic emeralds (Schmetzer *et al.*, 1997) and Nacken synthetic emeralds (this article), similar inclusions in two Chatham flux grown synthetic emeralds were also observed. These two faceted stones of 3.31 and 2.08 ct (*Figure 11*) from the Gübelin research collection are remarkable because they contain tiny crystals at the ends of elongate spicules without any contact to a special seed plate or to an irregularly shaped core.

In both synthetic emeralds, the microscopic examination in an immersion liquid revealed a pattern consisting of two distinct growth sectors which are related to the basal pinacoid and to a prism face (*Figure 12*). Numerous nailhead spicules were found as inclusions only in those growth sectors related to the basal pinacoid. The multicomponent inclusions consist of a birefringent tiny crystal at the widest ends of the elongate cone-shaped spicules, and colourless or yellowish, transparent or translucent substances within the cones; the spicules are oriented parallel to the *c*-axis (*Figure 13*).

Figure 12: *Growth pattern of Chatham synthetic emerald consisting of growth sectors related to the basal pinacoid (right) and to a prism face (left); nailhead spicules occur in the basal growth sector. The c-axis runs vertically, immersion, 50x.*

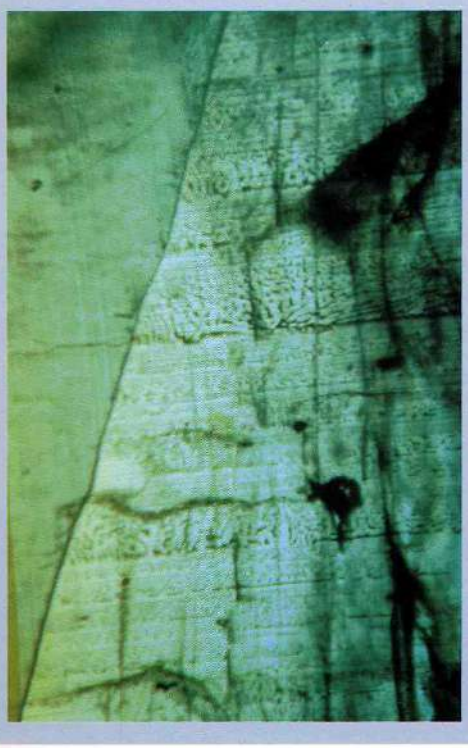

The examination of numerous birefringent crystals at the widest ends of the spicules by micro-Raman spectroscopy consistently indicated that they were phenakite. The spectra of the material trapped within the cones (*Figure 14*) consisted of several sharp Raman lines with the most intense and dominant lines

Figure 13: *Nailhead spicule with multi-component filling in Chatham synthetic emerald. 50x.*

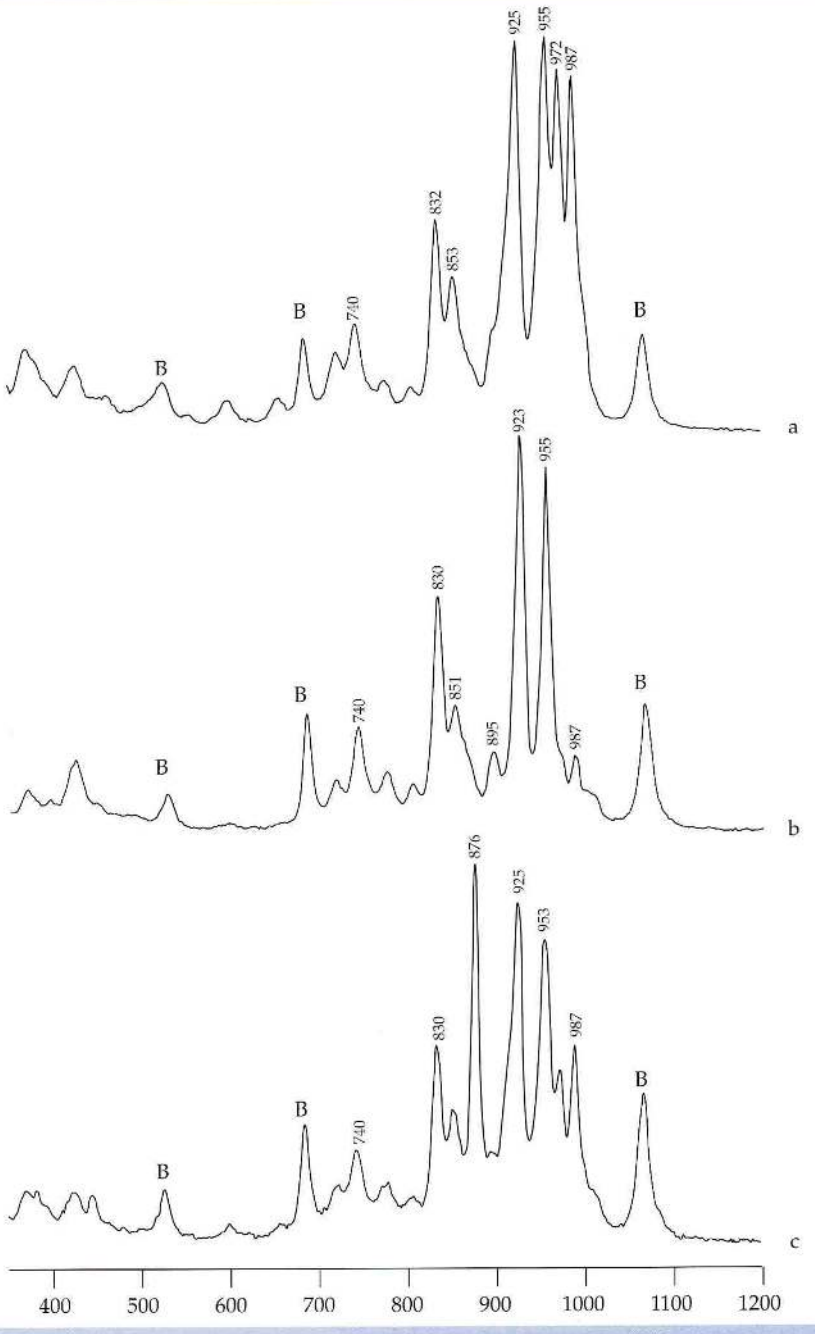

Figure 14: *Typical Raman spectra obtained from multiphase inclusions in spicules parallel to the c-axis of Chatham synthetic emerald crystals; the inclusions comprise residues of a molybdenum-bearing flux and components of beryl; the position of Raman lines of the host beryl is indicated by B, spectrum c shows the dominant Raman line of a phenakite nailhead at 876 cm^{-1}.*

always in the 900 to 1000 cm^{-1} range. In particular, four Raman lines at 925, 957, 972 and 989 cm^{-1} were frequently found in our spectra. Raman lines in the 430 and 830 cm^{-1} range were also present. Due to variable intensities of these dominant lines, probably different substances are trapped in the cone-shaped spicules of the two Chatham synthetic emeralds but some variation could be due to differences in orientation. This confirms conclusions drawn from microscopic examination (*Figure 13*). In both samples, the presence of molybdenum as a residual ingredient of the flux was proven by X-ray fluorescence (EDXRF).

At present, we are unable to present a complete and detailed interpretation of all Raman lines observed. However, comparing our measured Raman lines with literature data (Aveston *et al.*, 1964; Griffith and Lesniak, 1969; Johansson *et al.*, 1979; Kasprzak *et al.*, 1982; Murata and Ikeda, 1983, Schwab *et al.*, 1985; Ozeki *et al.*, 1987), we may conclude that several polymolybdates are present, especially the octomolybdate ion ($Mo_8O_{26}^{4-}$). In addition, the bands in the 830 and 430 cm^{-1} range are assigned to a polymerized network of SiO_4 tetrahedra and to isolated SiO_4 tetrahedra with non-bridging oxygen atoms.

(McMillan *et al.*, 1982; Xu *et al.*, 1989; Poe *et al.*, 1992). This strong Raman line is assigned to a three dimensional, polymerized Si–O–Si network or to six-membered Si–O–Si rings (McMillan *et al.*, 1982; Matson *et al.*, 1983; Xu *et al.*, 1989).

Raman spectra of Li_2O–SiO_2 and Li_2O–Al_2O_3–SiO_2 glasses have been examined by various authors. Glasses with lower Li_2O contents reveal strong Raman lines in the 490, 570, 950 and 1100 cm^{-1} ranges (Sharma and Simons, 1981; Matson *et al.*, 1983; Xu *et al.*, 1989; Fukumi *et al.*, 1990; Mysen, 1990; Mysen and Frantz, 1992); these were not observed in our spectra. Crystalline spodumene has two strong lines at 707 and 356 cm^{-1} (Sharma and Simons, 1981; Dowty, 1987), the 356 cm^{-1} line was not observed in our spectra. In Li_2O–SiO_2 glasses with higher Li_2O contents, however, a strong Raman line at 830 cm^{-1} is characteristic and is assigned to isolated SiO_4^{4-} tetrahedra (Iwamoto *et al.*, 1987; Tatsumisago *et al.*, 1987; Umesaki *et al.*, 1988). In these glasses, the SiO_4 tetrahedra contain non-bridging oxygen atoms. This assignment is confirmed by White and Minser (1984) for sodium silicate glasses.

Raman spectra of amorphous BeO show a strong line at 683 cm^{-1} and one weaker line at 723 cm^{-1} (Walrafen and Samanta, 1979). These two lines were also obtained from crystalline BeO, bromellite (Loh, 1968; Hofmeister *et al.*, 1987). Because the 683 cm^{-1} line is absent from some of our spectra showing a distinct 714 cm^{-1} line (see e.g. *Figure 10c*), an assignment of this line to BeO is rather uncertain.

According to the above data, a possible assignment of our Raman spectra obtained from trapped residual melt in Nacken synthetic emerald is as follows (see again *Figures 10a to f*):

component A, line at 956 cm^{-1} with a shoulder at about 871 cm^{-1} – polymerized polymolybdate, especially heptamolybdate;

component B, lines at 894 and about 317 cm^{-1} – non-polymerized molybdate;

component C, line at 430 cm^{-1} – polymerized Si–O–Si network or ring;

component D, line at 830 cm^{-1} – non-polymerized SiO_4 tetrahedra;

component E, line at 714 cm^{-1} – unknown component of the solidified (Li–Be)–Al–Si–V–Cr–Mo melt.

Most probably, the vanadium content of the residual melt is incorporated in components A to E, as has been already described for various hexamolybdates or molybdovanadophosphates (Kasprzak *et al.*, 1982; Buckley and Clark, 1985).

Consequently, the residual melt trapped in cavities of Nacken synthetic emerald consists of several components, the main

ones of which were identified as polymerized and non-polymerized molybdates, Si–O–Si networks and isolated SiO_4 tetrahedra. All components of the solidified melt are in the vitreous state and no crystalline phases have so far been identified. It is interesting to note that similar (Li–V–Mo) – (Be–Al–Si–Cr) – glasses were prepared as intermediate substances for the growth of synthetic emeralds (Kasuga, 1985 a, b, c, d, e). The variation of Raman spectra obtained from different parts of a single inclusion indicates that the melt trapped within such channels and spicules has partly unmixed during the cooling process. Similar observations,. i.e. phase separations in beryl glasses, have also been described by Riebling and Duke (1967).

At present, we are unable to assign the Raman line at 714 cm^{-1} to a specific crystalline or amorphous (vitreous) compound. Additional research is needed, and synthesis experiments should be performed to prepare specific compounds with known chemical compositions until one is found with this feature.

Conclusion

Nailhead spicules in Nacken synthetic emeralds consist of cone-shaped cavities with tiny crystals, most probably beryl, at the widest end and are partially filled with multicomponent inclusions. These inclusions derive from residual melt and consist of vanadium-bearing polymerized poly-molybdate and non-polymerized molybdate from vanadium- and molybdenum-bearing fluxes. Additional components of the solidified melt are isolated SiO_4 groups and polymerized aluminous silicates. It has been shown by optical, chemical and spectroscopic means that various cavities in Nacken synthetic emeralds contain single or multicomponent, partly inhomogeneous vitreous fillings. The fillings have partly unmixed during the final stage of emerald growth and subsequent cooling.

Acknowledgements

The authors are grateful to the following for supplying samples used in this study: Professor Dr E. Gübelin of Lucerne, Switzerland, Dr F.H. Pough of Reno, Nevada, USA, and M. Schaeffer of Detmold, Germany. Professor H.A. Hänni of Basel, Switzerland, kindly reviewed the manuscript.

References

Abello, L., Husson, E., Repelin, Y., and Lucazeau, G., 1983. Vibrational spectra and valence force field of crystalline V_2O_5. *Spectrochimica Acta*, **39A**(7), 641–51

Aveston, J., Anacker, E.W., and Johnson, J.S., 1964. Hydrolysis of molybdenum (VI). Ultracentrifugation, acidity measurements, and Raman spectra of polymolybdates. *Inorganic Chemistry*, **3**(5), 735–46

Badilescu, S., Boufker, K., Ashrit, P.V., Girouard, F.E., and Truong, V.-V., 1993. FT-IR/ATR study of lithium intercalation into molybdenum oxide thin film. *Applied Spectroscopy*, **47**(6), 749–52

Buckley, R.I., and Clark, R.J.H., 1985. Structural and electronic properties of some polymolybdates reducible to molybdenum blues. *Coordination Chemistry Reviews*, **65**, 167–218

Busey, R.H., and Keller, O.L., 1964. Structure of the aqueous pertechnetate ion by Raman and infrared spectroscopy. Raman and infrared spectra of crystalline $KTcO_4$, $KReO_4$, Na_2MoO_4, Na_2WO_4, $Na_2MoO_4.2H_2O$, and $Na_2WO_4.2H_2O$. *Journal of Chemical Physics*, **41**(1), 215–25

Cape, T.W., Maroni, V.A., Cunningham, P.T., and Bates, J.B., 1976. Raman and i.r.-emission studies of some tungstate- and molybdate-containing melts. *Spectrochimica Acta*, **32A**(5), 1219–23

Chowdari, B.V.R., Tan, K.L., and Chia, W.T., 1993. Structural and physical characterization of Li_2O:P_2O_5:MO_3 (M = Cr_2, Mo, W) ion conducting glasses. *Materials Research Symposium Proceedings*, **293**, 325–36

Clark, G.M., and Doyle, W.P., 1966. Infra-red spectra of anhydrous molybdates and tungstates. *Spectrochimica Acta*, **22**, 1441–7

Clauws, P., Broeckx, J., and Vennik, J., 1985. Lattice vibrations of V_2O_5. *Physica status solidi (b)*, **131**(2), 459–73

Delé-Dubois, M.-L., and Poirot, J.-P., 1989. Nature des inclusions dans les émeraudes suivant leurs origines. Georaman-89: Contributions, Symposium Université de Toulouse, France, Mai 1989, 8

Delé-Dubois, M.-L., Poirot, J.-P., and Schubnel, H.-J., 1986. Identification de micro-inclusions dans des rubis et émeraudes de synthèse par spectroscopie Raman. *Revue de Gemmologie a.f.g.*, **88**, 15–17

Dmitriev, I.A., and Khan, V.P., 1971. Formation of beryl structure in glasses of the BeO–Al_2O_3–SiO_2–MgO system. *Soviet Physics Crystallography*, 15(6), 1093–4

Dowty, E., 1987. Vibrational interactions of tetrahedra in silicate glasses and crystals: II. Calculations on melilites, pyroxenes, silica polymorphs and feldspars. *Physics and Chemistry of Minerals*, **14**, 128–38

Eppler, W.F., 1958. Synthetischer Smaragd. *Deutsche Goldschmiede-Zeitung*, **56**(4), 193–7

Espig, H., 1962. Die Synthese des Smaragdes und einiger anderer Minerale. *Berichte der Geologischen Gesellschaft der DDR*, **7**, 464–75

Feigelson, R.S., Martin, G.W., and Johnson, B.C., 1972. Crystal growth and properties of some alkali metal metavanadates. *Journal of Crystal Growth*, **13/14**, 686–92

Flanigen, E.M., Breck, D.W., Mumbach, N.R., and Taylor, A.M., 1967. Characteristics of synthetic emeralds. *American Mineralogist*, **52**(5–6), 744–72

Fukumi, K., Hayakawa, J., and Komiyama, T., 1990. Intensity of Raman band in silicate glasses. *Journal of Non-Crystalline Solids*, **119**(3), 297–302

Ghorai, A.K., and Bhattacharya, D.P., 1995. Mobility characteristics of non-equilibrium carriers in III–V compounds at low lattice temperatures. *Journal of the Physics and Chemistry of Solids*, **56**(2), 165–71

Goel, S.P., and Mehrotra, P.N., 1985. IR and thermal studies on lithium oxomolybdenum (VI) oxalate. *Journal of Thermal Analysis*, **30**, 145–51

Griffith, W.P., and Lesniak, P.J.B., 1969. Raman studies on species in aqueous solutions. Part III. Vanadates, molybdates, and tungstates. *Journal of the Chemical Society (a)*, **1969**, 1066–71

Hänni, H.A., Kiefert, L., Chalain, J.-P., and Wilcock, I.C., 1997. A Raman microscope in the gemmological laboratory: first experiences of application. *Journal of Gemmology.*, **25**(6), 394–406

Hirata, T., and Zhu, H.-Y., 1992. Identification and vibrational properties of the mixed oxide $(1-x)\ V_2O_5 + xMoO_3$ ($x \leq 0.3$). *Journal de Physique: Condensed Matter*, **4**(36), 7377–88

Hofmeister, A.M., Hoering, T.C., and Virgo, D., 1987. Vibrational spectroscopy of beryllium aluminosilicates: heat capacity calculations from band assignments. *Physics and Chemistry of Minerals*, **14**(3), 205–24

Iwamoto, N., Umesaki, N., Takahashi, M., Tatsumisago, M., Minami, T., and Matsui, Y., 1987. Molecular dynamics simulation of Li_4SiO_4 melt and glass. *Journal of Non-Crystalline Solids*, **95** and **96** (1), 233–40

Johansson, G., Pettersson, L., and Ingri, N., 1979. On the formation of hepta- and octa-molybdates in aqueous solution. X-ray scattering and Raman measurements. *Acta Chemica Scandinavica*, **A33**, 305–12

Kasprzak, M.S., Leroi, G.E., and Crouch, S.R., 1982. Raman spectroscopic investigation of isomeric and mixed-valence heteropolyanions. *Applied Spectroscopy*, **36**(3), 285–9

Kasuga, Y., 1985a. (Synthesis of single crystal of artificial beryl) [in Japanese]. Japanese Patent Application, Laid-Open No. 60–81084, May 9

Kasuga, Y., 1985b. (Synthesis of single crystal of artificial beryl) [in Japanese]. Japanese Patent Application, Laid-Open No. 60–81097, May 9

Kasuga, Y., 1985c. (Synthesis of single crystal of artificial beryl) [in Japanese]. Japanese Patent Application, Laid-Open No. 60–81098, May 9

Kasuga, Y., 1985d. (Synthesis of single crystal of artificial beryl) [in Japanese]. Japanese Patent Application, Laid-Open No. 60–81099, May 9

Kasuga, Y., 1985e. (Synthesis of single crystal of artificial beryl) [in Japanese]. Japanese Patent Application, Laid-Open No. 60–81100, May 9

Krasser, W., 1969. Die Ramanspektren von MoO_3 and WO_3. *Naturwissenschaften*, **56**(4), 213–14

Kurilenko, L.N., Serebryakova, N.V., Saunin, E.I., Gromov, V.V., and Sokolova, N.P., 1988. IR spectroscopy of the Li_2O–WO_3 and Li_2O–MoO_3 systems. *Bulletin of the Academy of Sciences of the USSR, Division of Chemical Science*, **37**, 839–44

Landais, E., 1971. Absorption du béryl dans le proche infrarouge. *Revue de Gemmologie a.f.g.*, **28**, 11–15

Landais, E., 1998. Personal communication

Loh, E., 1968. Optical phonons in BeO crystals. *Physical Review*, **166**(3), 673–8

Maaß, J., Ahrens, H., Fröbel, P., and Bärner, K., 1993. Raman spectra and cluster modes of some molybdate- and tungstate-borate glasses. *Solid State Communications*, **87**(6), 567–72

Matson, D.W., Sharma, S.K., and Philpotts, J.A., 1983. The structure of high-silica alkali-silicate glasses. A Raman spectroscopic investigation. *Journal of Non-Crystalline Solids*, **58**(2–3), 323–52

McMillan, P., and Piriou, B., 1982. The structure and vibrational spectra of crystals and glasses in the silica-alumina system. *Journal of Non-Crystalline Solids*, **53**, 279–98

McMillan, P., Piriou, B., and Navrotsky, A., 1982. A Raman spectroscopic study of glasses along the joins silica-calcium aluminate, silica-sodium aluminate, and silica-potassium aluminate. *Geochimica et Cosmochimica Acta*, **46**, 2021–37

Mysen, B.O., 1990. Role of Al in depolymerized, peralkaline aluminosilicate melts in the systems Li_2O–Al_2O_3–SiO_2, Na_2O–Al_2O_3–SiO_2, and K_2O–Al_2O_3–SiO_2. *American Mineralogist*, **75**, 120–34

Mysen, B.O., and Frantz, J.D., 1992. Raman spectroscopy of silicate melts at magmatic temperatures: Na_2–SiO_2, K_2O–SiO_2 and Li_2O–SiO_2 binary compositions in the temperature range 25–1475°C. *Chemical Geology*, **96**, 321–32

Nassau, K., 1976. Synthetic emerald: the confusing history and the current technologies. *Journal of Crystal Growth*, **35**, 211–22

Nassau, K., 1978. Did Professor Nacken ever grow hydrothermal emerald? *Journal of Gemmology*, **16**(1), 36–49

Nassau, K., 1980. *Gems made by man.* Chilton Book Company, Radnor, Pa., USA

Nassau, K., 1998. Personal communication

Nassau, K., and Nassau, J., 1980. The growth of synthetic and imitation gems. In: Freyhart, H.C. (Ed.), *Crystals. Growth, properties and applications. Vol. 2. Growth and properties.* Springer, Berlin, 1–50

Ozeki, T., Kihara, H., and Hikime, S., 1987. Studies of Raman spectra and equilibria of isopolymolybdate ions in aqueous acidic solutions by factor analysis. *Analytical Chemistry*, **59**(7), 945–50

Poe, B.T., McMillian, P.F., Angell, C.A., and Sato, R.K., 1992. Al and Si coordination in SiO_2–Al_2O_3 glasses and liquids: a study by NMR and IR spectroscopy and MD simulations. *Chemical Geology*, **96**, 334–49

Pope, S.J.A., and West, Y.D., 1995. Comparison of the FT Raman spectra of inorganic tetrahedral ions over the temperature range 77 to 473 K. *Spectrochimica Acta*, Part A, **51**(12),207–37

Py, M.A., Schmid, Ph.E., and Vallin, J.T., 1997. Raman scattering and structural properties of MoO_3. *Nuovo Cimento*, **38B**(2), 271–9

Riebling, E.F., and Duke, D.A., 1967. $BeO.Al_2O_3.SiO_2$ system: structural relationships of crystalline, glassy and molten beryl. *Journal of Materials Science*, **2**(1), 33–9

Sanchez., C., Livage, J., and Lucazeau, G., 1982. Infrared and Raman study of amorphous V_2O_5. *Journal of Raman Spectroscopy*, **12**(1), 68–72

Schmetzer, K., Bernhardt, H.-J., and Biehler, R., 1991. Emeralds from the Ural mountains, USSR. *Gems & Gemology*, **27**(2), 86–99

Schmetzer, K., and Kiefert, L., 1998. The colour of Igmerald: I.G. Farbenindustrie flux-grown synthetic emerald. *Journal of Gemmology*, **26**(3), 145–55

Schmetzer, K., Kiefert, L., Bernhardt, H-J., and Zhang B.L., 1997. Characterization of Chinese hydrothermal synthetic emerald. *Gems & Gemology*, **33**(4), 276–91

Schwab, S.D., McCreery, R.L., and Cummings, K.D., 1985. Effect of surface chemistry on the morphology, resistance and colloidal behaviour of small silver particles. *Journal of Applied Physics*, **58**(1), 355–60

Sharma, S.K., and Simons, B., 1981. Raman study of crystalline polymorphs and glasses of spodumene composition quenched from various pressures. *American Mineralogist*, **66**, 118–26

Spoliti, M., Cesaro, S.N., Bencivenni, L., D'Alessio, L., Enea, L., and Maltese, M., 1981. The infrared spectra of lithium, sodium, potassium and thallium chromates and lithium and cesium molybdates and tungstates. *High Temperature Science*, **14**, 11–16

Tang, S.H., Shen, Z.X., Ong, C.W., and Kuok, M.H., 1995. Raman spectroscopic study of $LiVO_3$ and $LiVO_3.2H_2O$. *Journal of Molecular Structure*, **354**(1), 29–35

Tatsumisago, M., Takahashi, M., Minami, T., Umesaki, N., and Iwamoto, N., 1987. Raman spectra of rapidly quenched Li_4SiO_4–Li_3BO_3 glasses. *Physics and Chemistry of Glasses*, **28**(2), 95–6

Umesaki, N., Iwamoto, N., Takahashi, M., Tasumisago, M., Minami, T., and Matsui, Y., 1988. Molecular dynamics study of Li_2O–SiO_2 melts and glasses. *Trans. Iron Steel Inst. Japan*, **28**(10), 852–9

Van Praagh, G., 1946. Synthetic emeralds. *Chemical Products and the Chemical News*, **9**, 10–11

Van Praagh, G., 1947. Synthetic quartz crystals. *Geological Magazine*, **84**, 98–100

Walrafen, G.E., and Samanta, S.R., 1979. Raman and infrared spectra of amorphous BeO and $Be(OH)_2.2H_2O$. *Applied Spectroscopy*, **33**(5), 524–5

Webster, R., 1955. The emerald. *Journal of Gemmology*, **5**(4), 185–221

Webster, R., 1958. Synthesis of emerald. *Gemmologist*, **27**(328), 203–6

Weinstock, N., Schulze, H., and Müller, A., 1973. Assignment of ν_2 (E) and ν_4 (F_2) of tetrahedral species by the calculation of the relative Raman intensities: the vibrational spectra of VO_4^{3-}, CrO_4^{2-}, MoO_4^{2-}, WO_4^{2-}, MnO_4^-, TcO_4^-, ReO_4^-, RuO_4, and OsO_4. *Journal of Chemical Physics*, **59**(9), 5063–7

White, W.B., and Minser, D.G., 1984. Raman spectra and structure of natural glasses. *Journal of Non-Crystalline Solids*, **67**(1–3), 45–59

Xu X., Li J., and Yao L., 1989. A study of glass structure in Li_2O–SiO_2 Li_2O–Al_2O_3–SiO_2 and Li–Al–Si–O–N systems. *Journal of Non-Crystalline Solids*, **112**(1–3), 80–4

Zhang, X., and Frech, R., 1997. Vibrational spectroscopic study of lithium vanadium pentoxides. *Electrochimica Acta*, **42**(3), 475–82

Zwaan, J.C., and Burke, E.A.J., 1998. Emeralds from Sandawana, Zimbabwe: the use of Raman microspectroscopy in identification of their solid inclusions. *Journal of Gemmology*, **26**(3), 174–87